IDENTIFYING ABNORMAL VEHICLE SUBCLASSES FROM WIM DATA FOR THE STRUCTURAL DESIGN OF HIGHWAY BRIDGES IN SOUTH AFRICA

J VAN ROOYEN[1] and PF VAN DER SPUY[2]

[1]Zutari (Pty) Ltd, 1 Century City Drive, Century City 7441; Tel: 066 287 3944;
Email: JacquesVR@zutari.com
[2]Department of Civil Engineering, Stellenbosch University, Private Bag X1, 7602;
Tel: 021 808 9111; Email: pierrevds@sun.ac.za

ABSTRACT

Abnormal vehicle loads pose significant detrimental effects when crossing bridges. By characterising the traffic load effects experienced on bridges caused by abnormal vehicles, allows for more reliable bridge design practices. This paper presents an innovative approach to identify and characterise subclasses of abnormal vehicle types from weigh-in-motion (WIM) data, by employing Gaussian Mixture Modelling to the load effects. Each subclass of abnormal vehicles has unique statistical properties and Gaussian distributions are utilised to determine characteristic load effects and reliability-based partial factors for each subclass. The aim of this paper is to characterise abnormal vehicles, and how this information can aid codified bridge design practises in the industry.

1. INTRODUCTION AND MOTIVATION

Technical Methods for Highways 7 (TMH7) is the current code of practice for the design of highway bridges in South Africa. The traffic load models were extracted from research done by Liebenberg in 1974 prior to the first publication in 1981. The code is based on CEB FIP Model Code for Concrete Structures of 1978, the British Code BS5400 and the National Building Code of Canada (Committee of State Road Authorities, 1981).

Information regarding the development of the code is limited and the incorporation of the abovementioned codes is thus unclear (Van der Spuy, 2020). After the initial publication in 1981, revisions were made to the code in 1988 which included the amendment of normal (NA) loading by increasing the distributed load by 6 kN/m and 20% axle load increase. However, Ullman (1988) and Oosthuizen et al. (1991) still found shortcomings in the traffic load model with specific reference to normal traffic on narrow and short span bridges, where TMH7 underestimates bending moments for spans between 4 m and 9 m, as well as shear forces for span lengths of up to 23 m. This led to further amendments including a 25% axle load increase.

In 1996, the South African National Department of Transport increased the legal limits of the gross vehicle weight (GVW) and the axle loads to 56 ton and 9 ton per axle, respectively. These changes were not implemented either. According to Van der Spuy (2020), the current TMH7 normal traffic load model is complicated to apply, which causes inconsistencies in the application thereof in practice. The TMH7 traffic load model therefore requires careful revision to represent current traffic characteristics. Research by Van der Spuy (2020) indicates that simply recalibrating the current TMH7 traffic load model would not be feasible. A possible alternative solution is to adopt the Eurocode

(EN 1991-2) load models in South Africa; however, Lenner et al. (2017) warned against the direct adoption, as vehicle characteristics in South Africa and Europe differ considerably.

In light of the complications highlighted above, Van der Spuy (2020) derived a new traffic load model using modern and novel techniques, based on current, real time traffic measurements obtained from site-specific permanent weigh-in-motion (WIM) data. Heavy vehicle traffic data recorded at the Roosboom permanent WIM station was used to calibrate the load model. The calibration was done using the characteristic load effects (LEs) derived from WIM data to determine a uniformly distributed load that is required to counter the truck point loads. These characteristic LEs are evaluated at a 975 year return period, which is based on a 5% probability of exceedance. Because of being within the port corridor with lots of commercial cargo, Roosboom, located on the N3 in KwaZulu-Natal, is reported to record the heaviest loaded vehicles in South Africa. The Roosboom WIM station is known to transport heavy freight between Durban ports to inland industrial locations such as the landlocked Gauteng Province, and especially the economic hub of Johannesburg. The newly derived traffic load model reduces the complexity of TMH7, but fails to recognise the difference in uncertainties between normal and abnormal traffic as Van der Spuy (2020) uses a mixture of vehicle types and characteristics when modelling the extreme load effects in the tail of the vehicle load statistical distribution. Therefore, whether these extreme LEs result from normal vehicles, illegally overloaded vehicles, or abnormal sized/loaded vehicles is unknown. Distinguishing between the LEs caused by normal and abnormal loaded vehicles is important as abnormal vehicles have different statistical properties that should potentially be treated in a separate abnormal load model.

The physical characteristics (dictating the statistical properties) of abnormal vehicles differs to normal vehicles and hence the LEs, will be distributed incompatibly. The interpretation of the magnitude of the LEs therefore differ between those associated with normal versus non-categorised abnormal vehicles. The statistical methods for determining the characteristic LEs differ fundamentally between normal and abnormal vehicles, primarily due to the considerable vehicle-specific properties, which directly influence the statistical parameters and their probability distributions.

It is, therefore, wise to distinguish between normal and abnormal vehicles when modelling traffic loads for the calibration of the bridge load models used in practice for codified designs. Although Van der Spuy (2020) reduces many complexities of the TMH7, it fails to recognise the difference in uncertainties between normal and abnormal traffic. By thoroughly investigating the characteristics of a pool consisting of different sub-populations of distinctive abnormal vehicles, i.e., pronounced vehicle-related properties that are inconsistent to normal vehicles, these uncertainties can be addressed. Consequently, by using vehicle-specific information (GVW, axle weights and configurations; and dimensional properties) to define a set of rules which identify abnormal vehicles from a WIM data set (i.e., by distinguishing these vehicles from normal vehicles), allows for abnormal vehicles to be properly characterised.

Characterising abnormal vehicles into unique abnormal vehicle types (sub-populations) is the primary requirement to effectively analyse abnormal vehicles, and hence, determine the characteristic LEs and reliability-based partial factors (PFs). This enables a thorough understanding of abnormal vehicles and the various types of abnormal vehicles, and their impact on bridges. A clear traffic loading description can be developed once abnormal vehicles are properly characterised, which increases the understanding of the LEs associated with them and leads to reduced uncertainties. This improved abnormal traffic

description and deeper understanding of their statistical properties enables for more advanced probabilistic LE modelling, increasing the resulting characteristic Les, and reliability-based PFs for the calibration of traffic load models.

2. STATISTICAL BACKGROUND

2.1 Relevant Probability Theory

A random variable, X, represents all the outcomes of a random experiment. The value x is unknown prior to the realisation of the event. A sample space, S, is a set which contains all the possible outcomes of X, which has only one value x. Random variables are either discrete or continuous. The sample space of discrete random variables is limited to a finite number of distinct values, whereas continuous random variables can take on any real value in a given interval (Holicky, 2009).

The continuity makes it impossible to assign meaningful probabilities to all the possible values within the interval of a continuous random variable. Probability distributions are specified instead. A distribution is defined by the cumulative distribution function (CDF), $F(x)$, where x can take on any value within X, which for a given value of X will give a value smaller than or equal to x as illustrated in Equation 1.

$$\boldsymbol{F(x) = P(X \leq x)} \tag{1}$$

The probability density function (PDF), $f(x)$, is equal to the first derivative of the probability distribution function given that it is differentiable. The probability that X attains a value in a given interval $[x_1;\ x_2]$ is formulated in Equation 2.

$$\boldsymbol{f(x) = \frac{dF(x)}{d(x)}} \tag{2}$$

2.2 Gaussian Distribution

The Gaussian distribution is a symmetrical distribution and the sample space of the random variable X is valid on the interval $-\infty < x < \infty$ (Coles, 2001). The distribution is described by two parameters, namely the mean (μ) and standard deviation (σ), with an infinite range for μ and $\sigma > 0$. As this is a symmetrical distribution, the skewness is zero, with the mean located at the centre and the dispersion dictated by the standard deviation.

2.3 Fundamental Concepts of Reliability

Structural reliability ultimately refers to the ability of a structure to safely resist an applied action and is based on the probability of structural failure over a specified period. ISO (2015) formally defines reliability *as the ability of a structural system or element to satisfy the design requirements (limit states) that are specified for its design period*, where limit states refer to the conditions that a structure must meet to fulfil its purpose. The two relevant limit states are the Serviceability Limit State (SLS) and Ultimate Limit State (ULS), respectively (Coles, 2001; Holicky, 2009).

Structural reliability is based on the requirement that the LE on a structure E does not exceed the structural resistance R, or $E < R$. The inequality $R \leq E$ thus defines a failure mode. The limit state function, Z, is formulated as $Z = R - E$ where R and E denote the modelled resistance and LE, respectively. The boundary between the safe and unsafe

domain is denoted by the limit state $Z = 0$, and failure of the particular limit state is denoted $Z \leq 0$. The probability of failure p_f is mathematically expressed as $p_f = P(E > R) = P(Z < 0)$, and the random variables E and R can be described by probability distributions (Holicky, 2009).

2.4 Partial Factors (PFs)

PFs are applied to the load and resistance, respectively, to ensure an adequate margin (β) by which structural resistance exceeds the applied loads (Schneider, 1997). The design load effects are determined by multiplying the characteristic LEs by PFs and are done for both SLS and ULS. The fib Bulletin 80 (Fib, 2016) describes the PF format as $\gamma_E = \gamma_{Ed,M}\gamma_e$, where γ_E and $\gamma_{Ed,M}$ are the PFs for the applied load and model uncertainty, respectively. The reliability-based PF γ_e accounts for traffic load variability and model-related uncertainties. Model uncertainty accounts for neglected effects when calculating LEs or simplifying assumptions in mathematical relations. The reliability-based PF γ_e is expressed as a ratio of the design LE and the characteristic LE denoted as E_d and E_c, respectively ($\gamma_e = \frac{E_d}{E_c}$).

3. SEQUENCIAL METHODOLOGY DEVELOPMENT

The statistical methodology approach followed to characterise abnormal vehicles into subclasses is based on a framework developed by Lenner and Sykora (2016), which investigates *Special Vehicles*. The framework is based on research by Lenner (2014), which investigated LEs that result from the passage of military vehicles over bridges in European and allied countries. Similarly to well-defined military vehicles being analogous to Special Vehicles, enabling the calibration of Lenner and Sykora (2016) by using the data from Lenner (2014), abnormal vehicles in this study are assumed analogous to Special Vehicles which allows for the framework by Lenner and Sykora (2016) to employed in this work.

3.1 Discussion of the Framework for Special Vehicles

It is common practice that civilian bridges in European and allied countries are occupied by military traffic. The use of these bridges is regulated according to the standards governed by the Standardised Agreement 21 (STANAG 21), and it is argued by Lenner (2014) that it lacks a defined safety concept and PFs to ensure reliable crossings of military vehicles over existing civilian bridges. To account for these shortcomings, Lenner (2014) investigates military loads to develop a suitable safety concept for the military assessment of existing bridges by establishing a framework to derive PFs and LEs for special vehicles on bridges.

The framework is based on the correlation between reduced uncertainties associated with well-defined heavy vehicles (Special Vehicles) and the PFs for these vehicles, which should be reduced accordingly. It suggests that the LEs due to the passage of a single well-defined vehicle (Special Vehicle) can be described with a higher degree of accuracy because there is less uncertainty than the LEs associated with a generalised traffic stream with a high degree of uncertainty. Military vehicles are examples of well-defined vehicles. The static LEs Q_{stat}, which includes measurement uncertainties due to the passage of special vehicles Q_{spec} is determined from the expression $Q_{spec} = \theta\delta Q_{stat}$, where θ and δ denote the model uncertainty associated with estimating the LEs and the dynamic amplification factor, respectively. The characteristic LEs for special vehicles $Q_{k,spec}$ is

determined as the product of the static LEs Q_{stat} and the random variables θ and δ, which are equal to their mean values as per Equation 3. The design LE for a special vehicle is proportional to the product of the characteristic LE $Q_{k,spec}$ and a relevant partial factor $\gamma_{Q_{spec}}$ as expressed in Equation 4.

$$\boldsymbol{Q_{k,spec} = \mu_{Q_{spec}} = \mu_{\theta}\mu_{\delta}\mu_{Q_{stat}}} \tag{3}$$

$$\mathrm{Q_{d,spec}} = \gamma_{\mathrm{Q_{spec}}}\mathrm{Q_{k,spec}} \tag{4}$$

The formulation of Equation 4 results from the assumption that $\gamma_{Q_{spec}}$, θ and δ are distributed lognormally. A lognormal distribution is suitable for Q_{spec}, regardless of a normally distributed Q_{stat}, due to the large variability associated with the random variables θ and δ. The parameters α_E and β denote the FORM sensitivity factor for the load and target reliability index, respectively. Equation 5 is used to estimate the coefficient of variation (COV) of Q_{spec}, denoted $V_{Q_{spec}}$. The parameter $V_{Q_{spec}}$ is calculated as per Equation 6.

$$\gamma_{Q_{spec}} = \frac{Q_{d,spec}}{Q_{k,spec}} = \frac{[\mu Q_{spec}\exp\left(-\alpha_E\beta V_{Q_{spec}}\right)]}{\mu_{Q_{spec}}} = \exp\left(-\alpha_E\beta V_{Q_{spec}}\right) \tag{5}$$

$$\boldsymbol{V_{Q_{spec}} \cong \sqrt{V_{\theta}^2 + V_{\delta}^2 + V_{Q_{spec}}^2}} \tag{6}$$

3.2 Evaluation of the Framework for Abnormal Vehicles

The framework is based on well-defined military vehicles, which are associated with low uncertainty. This low uncertainty directly affects the shape of the LE PDFs, which in turn dictates the 'distance' (measured as the *'number of standard deviations from the mean'*) between μ and the right-most position of the tail 3σ. A short distance between the statistical parameters μ and 3σ, i.e., narrow LE PDFs (which are clustered closely around the mean as shown by the dashed PDF in Figure 1), is a fundamental requirement of the framework and validates the primary assumption that $Q_{k,spec} = \mu_{Q_{spec}}$, which is inherently related to $\gamma_{Q_{spec}}$, $Q_{d,spec}$ and $Q_{k,spec}$.

The assumption that $Q_{k,spec} = \mu_{Q_{spec}}$ is dependent on the definition of Special Vehicles, defined as "*Authorised* [permit] *vehicles transporting heavy freight*" or "*A military vehicle in an emergency or crisis situation when responding to a threat is necessary*". Special Vehicle crossings are therefore rare events, i.e., not a general phenomenon. The assumption that $Q_{k,spec} = \mu_{Q_{spec}}$ suggests that 50% of vehicles will exceed the characteristic load $Q_{k,spec}$. The assumption that $Q_{k,spec} = \mu_{Q_{spec}}$ can be argued to be reliable and safe due to the rare occurrence of single, Special Vehicle crossings (50% chance of exceeding SLS limits). However, this is not true for general traffic flow conditions consisting of a mixture of normal and abnormal vehicles. The dashed PDF in Figure 1 represents single crossing events of well-defined special vehicles as per the above definition and is associated with low uncertainty. The PDF will have a low COV proportional to the low degree of dispersion around the mean μ, and hence low PFs given that the PFs are directly related to the COV as per Equations 5 and 6.

The primary difference between abnormal vehicles and Special Vehicles is that abnormal vehicles have a considerably higher frequency of occurrence. When considering the PDF representing abnormal LEs (depicted by the solid line in Figure 1), there is significant dispersion around the mean μ. The high standard deviation σ suggests that abnormal vehicles are expected to have an increased COV, ranging between the upper-medium (best case, rare) to high (worst case, most likely) density.

In comparison to the case of Special Vehicles, the distance between the mean μ and the extreme right tail at 3σ is significantly inflated, in contrast to the short distance between μ and 3σ for Special Vehicles. The assumption that $Q_{k,spec} = \mu_{Q_{spec}}$ is thus not valid for abnormal vehicles due to the high frequency of abnormal vehicle crossings and the high degree of dispersion, which significantly increases the likelihood that the characteristic LE is exceeded.

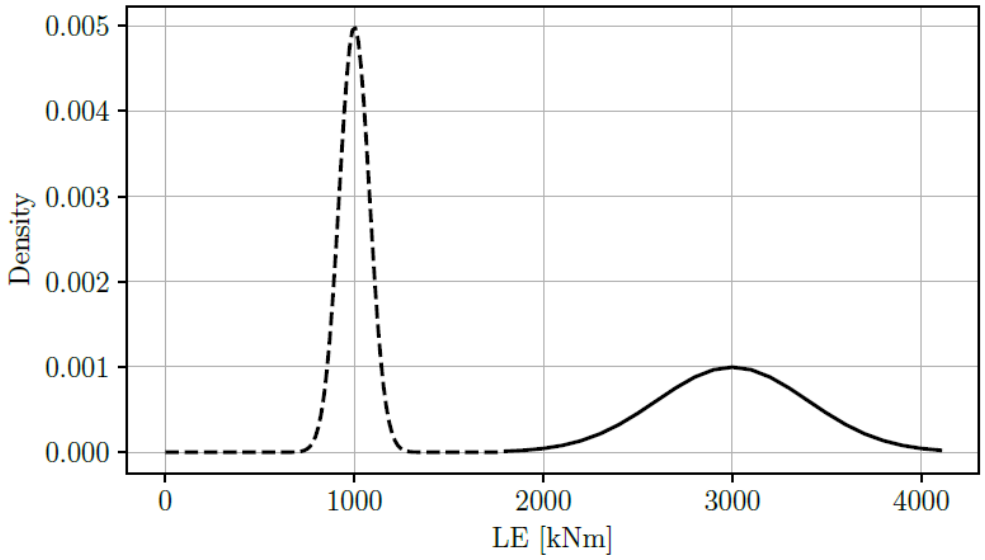

Figure 1: Difference in PDF shape of European military data (dashed line) versus South African data (solid line)

4. METHODOLOGY

4.1 Abnormal Vehicle Subsets

Abnormal vehicle subclasses are identified in a two-step process. The primary step considers abnormal vehicles holistically, by which abnormal vehicles are assigned to subclasses based solely on the number of axles. In this step, subclasses are established based solely on the number of axles, with the assumption that abnormal vehicles have more than seven axles. Vehicles with fewer than seven axles (axles≤ 7) are considered normal vehicles. This assumption is based on the proportion of vehicles that occur on the South African national roads and the relevant legislation as per the National Road Traffic Regulation (NRTR, 1999). Hence subclasses of eight and nine-axle vehicles are considered. Furthermore, it is argued that there exist abnormal vehicles (having more than seven axles) having gross vehicle weight (GVW) less than the legal limits (56 ton) in South Africa and therefore, in the primary step, hence the subclasses have no upper and lower bounds for the GVW limitations and thus containing all abnormal vehicles from all valid GVW groups (1kN+). The absence of GVW limits when subclasses are established relates to the fact that vehicle abnormality is related to both, weight abnormalities (extremely

heavy vehicles) and dimensional abnormalities (unusual axle configurations and vehicle dimensions). These eight- and nine-axle vehicles comprise different underlying abnormal vehicle types, which are unique and have vehicle-specific characteristics which separate them from the other groups. The characterisation is based on the Gaussian mixture modelling (GMM) (Steenbergen & Morales Napoles, 2012; Zhang & Huang, 2015).

Abnormal vehicle subclasses are not limited to eight and nine-axle vehicles (as in this paper) and can extend beyond nine axles. However, eight and nine-axle vehicles are the most common abnormal vehicles recorded at the WIM station used in this study and thus dominate in occurrence frequency on the South African highways. Sufficient data points are available for these vehicles, allowing reliable statistical analyses and a high degree of confidence in the results. Vehicles with more than nine axles fall beyond the scope of this study.

The characterisation of abnormal vehicle subclasses is explained as follows: consider the hogging moments resulting from eight axle abnormal vehicles on a 30 m span in the Limpopo province, which is graphically depicted by the histogram in Figure 2. The histogram is trimodal as three modes exist (’peaks’). Each mode represents a unique, abnormal vehicle subclass type that exists within the eight-axle subclass. These modes, each representing an abnormal vehicle type (in the general case, either eight axle or nine axle vehicles, or more than nine axles), are individually isolated and statistically analysed by fitting a normal distribution to each of the individual modes. This is done by employing the GMM, a statistical method by which independent normal distributions are fit to each mode, as shown by the blue, green, and red PDFs on the respective modes of the LE histogram in Figure 2.

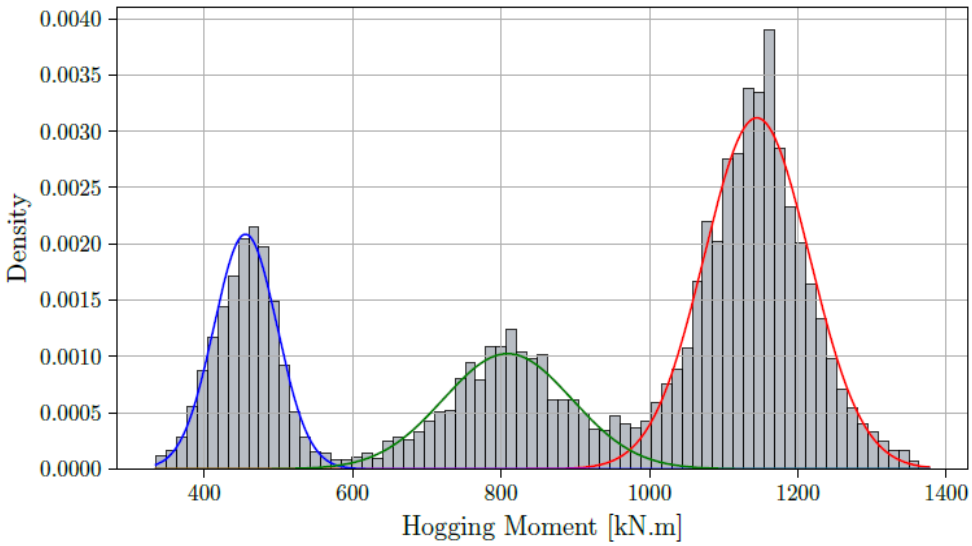

Figure 2: Trimodal histogram of abnormal vehicle LEs and respective GMM PDFs

4.2 Deriving LEs and PFs for Abnormal Vehicles

An increased standard deviation of the LEs is associated with abnormal vehicles, which correlates with the higher variability of abnormal vehicles (as opposed to well-defined and managed military or special vehicles). The increased standard deviation invalidates the assumption that $Q_{k,ab} = \mu_{Q_{ab}}$ and must therefore be modified to account for the dispersed data points not being concentrated about the mean (μ).

The characteristic LEs for abnormal vehicles are evaluated at the 95th percentile value, which is positioned at 1.645 standard deviations (1.645σ) away from the mean μ (within the right tail region of the normal distribution) as per Equation 7. This is per the discussions in Section 3.1 where the issue was raised regarding the increased adverse influence of 50% of the abnormal vehicles that exceed the magnitude of characteristic LEs (as opposed to Special Vehicles) when evaluated according to $Q_{k,ab} = \mu_{Q_{ab}}$ (which is not a valid assumption when analysing abnormal vehicles).

$$Q_{k,ab} = \mu_{Q_{ab}} + 1.645 \tag{7}$$

Consider the red PDF in Figure 2, which shows the isolated normal distribution of the third mode of the histogram after employing GMM. The isolated normal distribution is independent of the normal distributions associated with the other modes (green and blue PDFs). The characteristic LE, e.g., hogging moment M_C, associated with each mode is individually evaluated at the 95th percentile using Equation 7 as $M_{C,95} = \mu_{M,ab} + 1.645$. The same is true for sagging moments and shear forces. The parameter $\mu_{M_{ab}}$ is the mean and σ is the standard deviation of the static hogging moments, respectively. The PF is a ratio between the design LE (E_d) and the characteristic LE (E_c), where the design LE is the inverse CDF of the static LEs Q_{stat} associated with the isolated mode and is calculated using Equation 8.

$$\gamma_e = \frac{M_d}{M_{C,95}} \tag{8}$$

$$M_d = F_{X,t_{ref}}^{-1}\left[\Phi(\alpha\beta), t_{ref}\right] \tag{9}$$

$F_{X,t_{ref}}^{-1}$ is the inverse standard normal distribution of the static LEs Q_{stat} over a reference period t_{ref}. This is true for all LEs (hogging moments, sagging moments, and shear forces) for any mode. This study is limited to ULS PFs, and therefore $\beta_{T,ULS} = 3.5$, as recommended in Van der Spuy (2020). The FORM sensitivity factor is $\alpha_E = -0.7$, as recommended for the dominant variables in EN 1990 (CEN, 2002) and IS02394 (ISO, 2015). The return period for ULS, T_{ULS} is thus calculated as:

$$T_{ULS} = \frac{t_{ref}}{p} = \frac{t_{ref}}{\phi(\alpha_E \beta_{T,ULS})} = \frac{100}{\phi(-0.7\times 3.5)} = 5040 \text{ years} \tag{10}$$

The ULS probability of non-exceedance p_{ULS} is calculated to evaluate the design quantiles:

$$p_{ULS} = 1 - \frac{1}{T_{ULS}} = 1 - \frac{1}{5040} = 0.9998 \tag{11}$$

By substituting the above values into Equation 9, the design quantile is then calculated as:

$$M_d = F_{X,t_{ref}}^{-1}[\Phi(-0.7 \times 3.5), p_{ULS} = 0.9998] \tag{12}$$

5. APPLICATION TO SOUTH AFRICAN DATA

5.1 Calculating the Load Effects

The LE data used in the methodology discussed above is the result of processed WIM data as per Van Der Spuy (2020). Firstly, raw WIM data recorded in the nine South African

provinces is cleaned and calibrated. Filtering techniques are employed to omit all eight and nine axle vehicles (as per the primary subclass based only on the number of axles, discussed in Section 4.1). The cleaned and calibrated data records of these eight- and nine axle vehicles contain information including time stamps, vehicle speed, axle weights, and spacing.

The time stamps and speeds are used to calculate the distance between vehicles and to assemble a convoy of vehicles. The distance between the rear axle of the front vehicle and the front axle on the following vehicle is calculated by using time difference and speed. Simplified studies utilise a single-vehicle analysis (Nowak & Hong, 1991; Nowak, 1994; Anderson, 2006), but the South African data has satisfactory accuracy for continuous convoys. According to De Wet (2010b), WIM errors in South Africa are generally less than 10%. The vehicle convoys are a series of point loads and distances, which represent actual vehicles, are incrementally passed over varying span lengths between 5 m and 30 m to calculate the different LEs (sagging moments, hogging moments and shear forces) using simple principles of statics and influence lines. The maximum values for each LE and span length are recorded for the abnormal vehicles.

5.2 Abnormal Vehicle Characterisation

By investigating the static LEs, which are caused by the subsets of abnormal vehicles (eight-axle and nine-axle vehicles), it is found that the modality of the datasets, and hence the number of abnormal vehicle types, vary in the nature of the LEs (sagging moments, hogging moments and shear forces) based on the number of axles.

For example, the LEs caused by the eight-axle vehicle subset in Mpumalanga is trimodal (i.e., three abnormal vehicle types), whereas the LEs caused by the nine-axle vehicle subset, also in Mpumalanga, has only one mode (i.e., one abnormal vehicle type). Although the modality of the LEs vary for the respective subsets, it remains consistent with the nature of the LEs. In Mpumalanga, the LEs of eight-axle vehicles is trimodal for sagging moments, hogging moments and shear forces. The LEs of nine-axle vehicles have one mode for sagging moments, hogging moments, and shear forces, which is prevalent at all the WIM stations studied.

As a result, the characteristic LEs are determined for each abnormal vehicle type within the eight and nine-axle vehicle subsets based on the modality of the respective subsets. Table 1 provides a summary of the number of abnormal vehicle types associated with eight- and nine-axle abnormal vehicles, respectively. Hence, the characteristic LEs and reliability-based PFs will be determined for each abnormal vehicle type, based on the association with abnormal vehicles with eight- and nine-axles, respectively.

Table 1: Number of abnormal vehicle types (sub-populations) associated with eight-and nine axle abnormal vehicles, consistent for each LE (hogging, sagging and shear) per axle group (eight, nine axle abnormals)

Province → / Vehicle type ↓	WC	EC	FS	GP	KZN	LP	MP	NC	NW
8-axle abnormal vehicle	3	3	2	2	2	3	3	2	2
9-axle abnormal vehicle	2	1	2	3	2	1	1	2	3

Legend: WC = Western Cape; EC = Eastern Cape; FS = Free State; GP = Gauteng Province; KZN = KwaZulu-Natal; LP = Limpopo Province; MP = Mpumalanga; NC = Northern Cape; NW = North West

5.3 Characteristic LEs and PFs due to South African Abnormal Vehicles

The approach to computing characteristic LEs and reliability-based PFs from static LEs is demonstrated in this section with an example that utilises static LEs Q_{stat} (hogging moments in this case), which result from incrementally moving eight-axle abnormal vehicles on a 20 m span length in Limpopo. Figure 2 presented earlier in this paper shows a histogram LEs. Given the tri-modality of the dataset and Q_{stat} distributed normally, isolating each of the three modes by employing GMM permits statistical computations of the three independent normal distributions individually. Each of the three individual normal distributions represents unique types of abnormal vehicles (each type unique to eight-axle abnormal vehicles). The vehicles associated with the LEs in the first mode in Figure 2 are statistically analysed by the normal distribution associated with the blue PDF. They are characterised as *Type 1* vehicles. The same process is followed for the first and second modes. The isolated normal distribution for *Type 1* vehicles has statistical parameters μ = 339.86 kNm and σ = 39.39 kNm, with a COV = 0.092. The characteristic hogging moment M_C for the abnormal vehicle subset is:

$$M_C = \mu_{Q_{ab}} + 1.645\sigma = 340 + 1.645 \times 39 = 404\text{kNm} \tag{13}$$

The design value M_d is then calculated using Equation 9.

$$M_d = F^{-1}_{X,t_{ref}}[\Phi(-0.7 \times 3.5), p_{ULS} = 0.9998] = 479\text{kNm} \tag{14}$$

This leads to computing the reliability-based PF as the ratio between the design and characteristic hogging moments, $\gamma_e = \frac{M_d}{M_C} = \frac{479}{404} = 1.2$.

6. RESULTS AND DISCUSSION

The procedure discussed in the previous section was followed to determine the LEs (hogging moments, sagging moments, and shear forces) and the associated reliability-based PFs for the characterised eight- and nine axle abnormal vehicles subclasses (*Type 1, Type 2,* and *Type 3*) in each province. Abnormal vehicles comprising the first peak of bi-modal and tri-modal (*Type 1* vehicles) result from unloaded abnormal or a mixed traffic stream of normal and abnormal vehicles. These vehicles are typically not well-defined and have larger PFs, which is related to increased uncertainty in the vehicle and statistical properties and hence, the LEs.

Type 1 abnormal vehicles are likely to form part of the threshold between normal and abnormal vehicles, referred to as threshold vehicles. Threshold vehicles are not as well-defined as normal and abnormal vehicles, which further explains the inconsistent loading and underlying distributions. *Type 2* abnormal vehicles exhibit similar behaviour but to a lesser extent than *Type 1* abnormal vehicles. Opposite to *Type 1* abnormal vehicles, which may be associated with empty trucks, *Type 3* abnormal vehicles may be subject to the same rationale by representing fully laden vehicles.

For sagging moments resulting from eight-axle trucks with tri-modal properties, it was found that the second mode (*Type 2* vehicles) often has the largest PFs and typically exhibits a high degree of inter-provincial variation. This phenomenon is analogous to the principle of threshold vehicles. Here, the second mode comprises vehicles with significant vehicular differences (such as axle configuration, less advanced levelling, etc.); hence, the LEs are statistically inconsistent and nonconforming to a particular statistical distribution.

Like threshold vehicles (neither normal nor abnormal), these vehicles are neither *Type 1* nor *Type 2*, and hence, a significant degree of variation exists among the vehicle types responsible for the LEs of the second mode.

In light of the above, consider the sagging moments by eight-axle abnormal vehicles in Limpopo, which has a tri-model LE histogram and hence, three abnormal vehicle sub-classes. The largest PFs are associated with *Type 2* abnormal vehicles and the lowest PFs with *Type 3* abnormal vehicles. Consider Figure 2, showing the multimodal histogram and normal distributions for each mode for sagging moments on a 20 m span length in Limpopo. It shows how the blue and red Gaussian distributions (*Type 1* and *Type 3* subclasses) have a narrower shape than the green Gaussian distribution (*Type 2* subclass).

Focusing on the second and third modes in Figure 2, it is hard to define a clear boundary (or threshold) between the right tail of the second mode and the left tail of the third mode. This ambiguity significantly affects the PFs as the Gaussian PDFs are influenced by this overlapping, decreasing the goodness of fit. This phenomenon is true for three of the four provinces (Mpumalanga, Eastern Cape, Western Cape, and Limpopo) that have tri-modal sagging moment histograms. The exception is Mpumalanga, and the largest PFs are associated with the *Type 1* subclass. Mpumalanga also has the largest PF of 1.279 for sagging moments at a span length of 10 m. This is also true for hogging moments and shear forces for eight-axle abnormal vehicles as the modality is the same for all LEs (hogging moments, sagging moments and shear forces) of a specific abnormal vehicle subclass (eight- and nine-axle abnormal vehicles).

Figure 3 shows the multimodal histogram for sagging moments in the Eastern Cape. The narrow-shaped red PDF, isolated by employing GMM, agrees with the above discussions about the correlation between narrow shaped PDFs and low PFs for well-defined vehicles. The difference here is that the first mode (*Type 1* abnormal vehicles) is indeed well-defined, suggesting a predominant occurrence of either empty, well-defined abnormal vehicles, or a mixture of normal and abnormal vehicles with similar properties. The same explanation holds for the Western Cape.

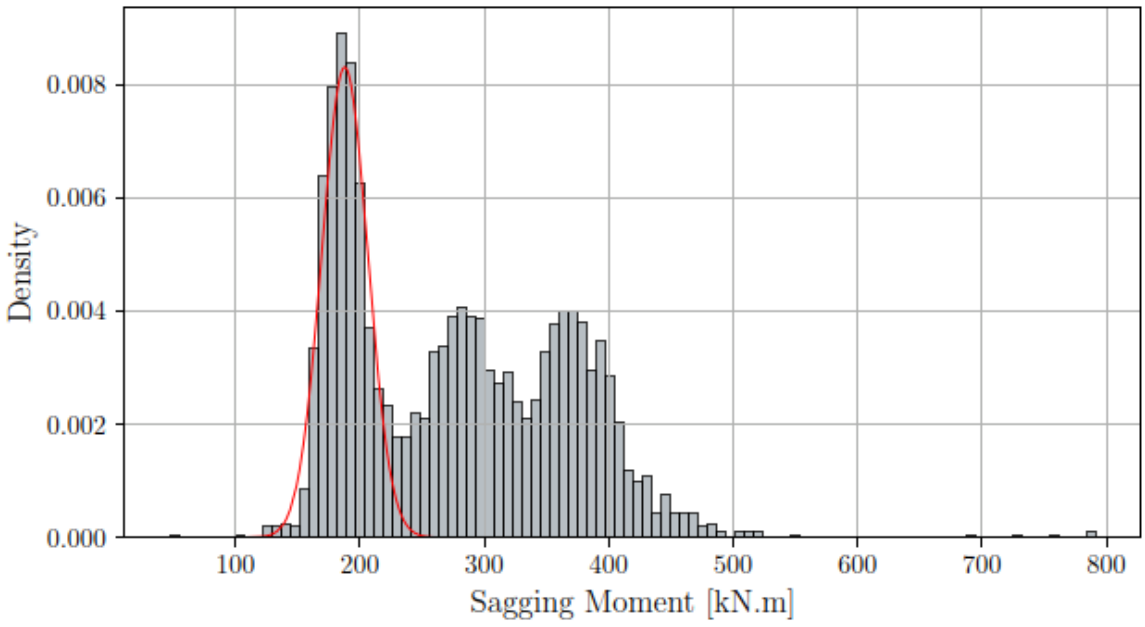

Figure 3: Histogram of sagging moments in the Eastern Cape showing a narrow-shaped Gaussian distribution fit to the first mode

Figure 4 holistically shows the reliability-based PFs for the LEs that result from eight- axle vehicles with three modes for all nine provinces. PFs associated with sagging moments are considerably lower than those of hogging moments and shear forces. The largest top 10% of all the PFs are associated with *Type 1* vehicles in Mpumalanga and *Type 2* vehicles in the Western Cape, with Mpumalanga governing the PFs overall. The PFs in the lowest 10% of all the PFs are primarily associated with *Type 3* vehicles (78% *Type 3* and 22% *Type 1*).

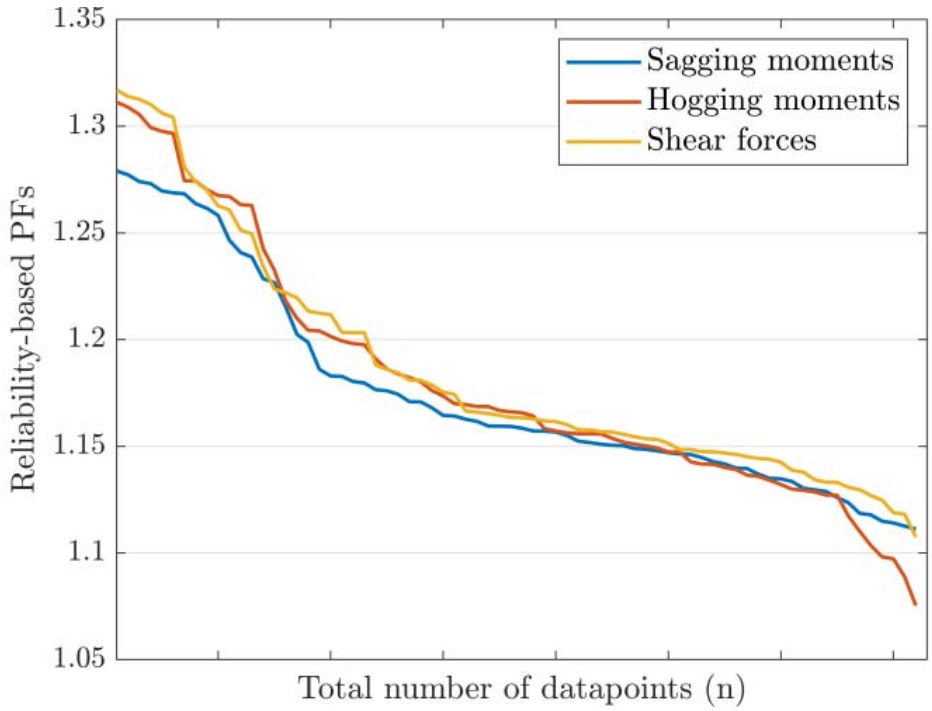

Figure 4: Reliability-based PFs for tri-modal LEs of eight-axle vehicles in each of the nine provinces

The characteristic sagging moments that result from eight-axle vehicles have negligible inter-provincial variation, with the LE magnitudes being almost similar for each span length. The magnitudes increase at the same trend as the span length increases. This is not the case considering the sagging moments resulting from nine-axle vehicles showing significant inter-provincial variation for all span lengths. A notable finding is that the variation between characteristic LEs and design LEs is also more significant for nine-axle vehicles than for eight-axle vehicles. This is true for hogging moments and shear forces.

The hogging moments that result from eight-axle vehicles show minor inter-provincial variation as opposed to those resulting from nine-axle vehicles. Hogging moments resulting from eight-axle vehicles are consistent between span lengths of 5 m and 15 m and exhibit less consistency for span lengths greater than 15 m. This is because entire vehicles able to occupy the bridge at longer, and therefore the GVW starts governing. Western Cape experiences considerably larger hogging moments resulting from nine-axle vehicles, whereas Mpumalanga and the Eastern Cape experience hogging moment LEs well below the other provinces, which is depicted in Figure 5. A possible explanation may be related to the abnormal vehicle subclasses, as the LE histograms associated with the nine-axle vehicles are unimodal in both Mpumalanga and in the Eastern Cape and relates to the earlier discussions of *Type 1* vehicles needing better definition.

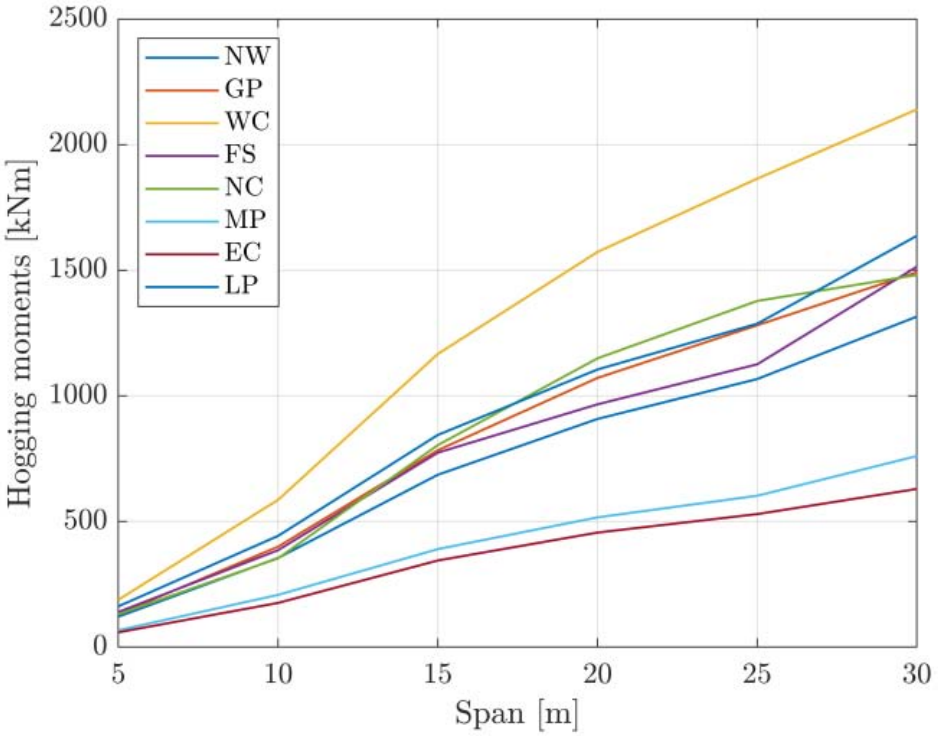

Figure 5: Maximum characteristic hogging moments resulting from nine-axle vehicles

7. CONCLUSION

This paper revealed the existence of different abnormal vehicle subclasses and showed that these vehicles influence the characteristic LEs and PFs. The characteristic LEs resulting from these subclasses show a considerably higher degree of inter-provincial variation associated with nine-axle vehicles than eight-axle vehicles. The scope of this study was limited to eight and nine-axle vehicles, and the influence of vehicles with more than nine axles is therefore unknown. The differences between the LEs that result from eight-axle vehicles compared to nine-axle vehicles could not be extended to vehicles with more than nine axles and are subject to further investigation.

The results from investigating the subclasses of eight and nine-axle vehicles suggest the possibility that characteristic LEs caused by abnormal vehicles are better treated individually when designing bridges in South Africa. In the context of this study, it implies that if abnormal vehicles are to be treated separately, it should be done on a case-specific basis by considering parameters such as average daily truck traffic, typical abnormal vehicle characteristics, and the holistic governing traffic flow characteristics that show dominance in specific regions. This research contributes to practice by introducing a novel methodology which can be applied to distinguish between the LEs induced by normal vehicles as opposed to those by abnormal vehicles. These characterised LEs assist in developing well-defined load models for the structural design of highway bridges in South Africa. The methodology developed in this work further contributes significantly to the technical realm by introducing a novel technique of analysing LEs experienced on bridges, which can be replicated in other countries and regions.

8. REFERENCES

Anderson, JRB. 2006. Review of South African Live Load.

Caprani CC. 2005 Probabilistic Analysis of Highway Bridge Traffic Loading. University College Dublin. PhD Thesis (2005).

CEN. 2002. EN1991-1: General actions for buildings, Tech. Rep., Brussels.

Coles, SG. 2001. An introduction to Statistical Modelling of Extreme Values. Springer, London. ISBN 1852334592. arXiv:1011.1669v3.

Committee of State Road Authorities. 1981. TMH7 Parts 1 and 2: Code of Practice for the Design of Highway Bridges and Culverts in South Africa. Tech. Rep.

Fib. 2016. Partial factor methods for existing concrete structures - Bulletin 80. Tech. Rep., Fédération internationale du béton, Lausanne.

Holicky. 2009. Reliability analysis for structural design. 1st edn. SUN meDIA, Stellenbosch.

ISO. 2015 General Principles on Reliability for Structures ISO2394, Tech. Rep., ISO, Geneva.

Lenner, R. 2014. Safety Concept and Partial Factors for Military Assessment of Existing Concrete Bridges.

Lenner, R & Sýkora, M. 2016. Partial factors for loads due to special vehicles on road bridges. Engineering Structures, 106:137-146. ISSN 18737323.

Models for Traffic Loading on Bridge and Culvert Structures Using WIM Data., University of Cape Town. Masters Thesis.

Nowak, AS. 1994. Load model for highway bridges, Structural Safety, 13(1-2):53-66.

Nowak, AS & Hong, Y. 1991. Bridge Live-Load Models, Journal of Structural Engineering, 117(9):2757-2767.

Steenbergen, RDJM & Morales Napoles, O. 2012. Traffic Load Model Based on Weigh-In-Motion Measurements. In Vol. 2 11th International Probabilistic Safety Assessment and Management Conference and the Annual European Safety and Reliability Conference 2012, PSAM11 ESREL 2012, 933-945.

Van der Spuy PF. 2020. Derivation of a traffic load model for the structural design of highway bridges in South Africa., Stellenbosch University. PhD Thesis 2020.

Zhang, H & Huang, Y. 2015. Finite Mixture Models and Their Applications: A Review. Austin Biom and Biostat. Austin Biom and Biostat, 2(2):1013-1.